Maximum Power Tracking for Photovoltaic Power Systems

Joe-Air Jiang[1], Tsong-Liang Huang[2], Ying-Tung Hsiao[2]* and Chia-Hong Chen[2]

[1]*Department of Bio-Industrial Mechatronics Engineering, National Taiwan University*
Taipei, Taiwan 106, R.O.C.
[2]*Department of Electric Engineering, Tamkang University*
Tamsui, Taiwan 251, R.O.C.

Abstract

The electric power supplied by a photovoltaic power generation system depends on the solar radiation and temperature. Designing efficient PV systems heavily emphasizes to track the maximum power operating point. This work develops a novel three-point weight comparison method that avoids the oscillation problem of the perturbation and observation algorithm which is often employed to track the maximum power point. Furthermore, a low cost control unit is developed, based on a single chip to adjust the output voltage of the solar cell array. Finally, experimental results confirm the superior performance of the proposed method.

***Key Words*:** Photovoltaic, Perturbation and Observation Algorithm, Maximum Power Point Tracking

1. Introduction

Photovoltaic (PV) generation is becoming increasingly important as a renewable source since it offers many advantages such as incurring no fuel costs, not being polluting, requiring little maintenance, and emitting no noise, among others. PV modules still have relatively low conversion efficiency; therefore, controlling maximum power point tracking (MPPT) for the solar array is essential in a PV system.

The amount of power generated by a PV depends on the operating voltage of the array. A PV's maximum power point (MPP) varies with solar insulation and temperature. Its V-I and V-P characteristic curves specify a unique operating point at which maximum possible power is delivered. At the MPP, the PV operates at its highest efficiency. Therefore, many methods have been developed to determine MPPT. For example: Ibrahimm and Houssing employed the look-up table on a microcomputer, to track MPP [1]. Midya et al. applied a dynamic MPP tracker to PV appliances [2]. Enslin and Snymam suggested the concept of "perturb and observe" (P&O) [3], alternatives to which have been recently presented [4,5]. Koutroulis et al. [6] and Hussein et al. [7] offered the incremental conductance (IncCond) technique, since when, enhanced IncCond techniques have been proposed [8,9]. Several investigations have recently applied fuzzy logic to resolve this problem [10,11].

In MPPT, most control schema use the P&O technique because it is easy to implement. But the oscillation problem is unavoidable. This research developed an extended P&O technique - a three-point weight comparison method based on an 8-bit single-chip control unit - by utilizing a boost converter to adjust the output voltage of the PV for tracking the MPP. Models and simulations of this PV system and MPPT algorithms are offered with experimental results.

The rest of this paper is organized as follows. Section II introduces the basic principle of the PV system. Sections III and IV describe the traditional P&O and the proposed algorithm three-point weight comparison method, respectively. Section V shows the configuration of the proposed PV system. Section VI discusses experimental results as illustrations. Conclusions are finally drawn in

*Corresponding author. E-mail: hsiao@mail.tku.edu.tw

the last section.

2. Mathematical Model

The building block of PV arrays is the solar cell, which is basically a p-n semiconductor junction, shown in Figure 1. The V-I characteristic of a solar array is given by Eq. (1) [4].

$$I = I_{SC} - I_O \left\{ \exp\left[\frac{q(V + R_S I)}{nkT_k} \right] - 1 \right\} - \frac{V + R_S I}{R_{sh}} \quad (1)$$

where V and I represent the output voltage and current of the PV, respectively; R_s and R_{sh} are the series and shunt *resistance* of the cell; q is the electronic charge; I_{SC} is the light-generated current; I_o is the reverse saturation current; n is a dimensionless factor; k is the Boltzman constant, and T_k is the temperature in ^{o}K.

Equation (1) was used in computer simulations to obtain the output characteristics of a solar cell, as shown in Figure 2. This curve clearly shows that the output characteristics of a solar cell are non-linear and are crucially influenced by solar radiation, temperature and load condition. Each curve has a MPP, at which the solar array operates most efficiently.

3. Maximum Power Point Tracking

Several techniques for tracking MPP have been proposed, as described in Section I. Two algorithms are commonly used to track the MPPT - the P&O method and IncCond method. The P&O method has been broadly used because it is easy to implement. Figure 3 presents the control flow chart of the P&O algorithm. The MPP tracker operates by periodically incrementing or decrementing the solar array voltage. If a given perturbation leads to an increase (decrease) the output power of the PV, then the subsequent perturbation is generated in the same (opposite) direction. In Figure 3, *set Duty out* denotes the pertur-

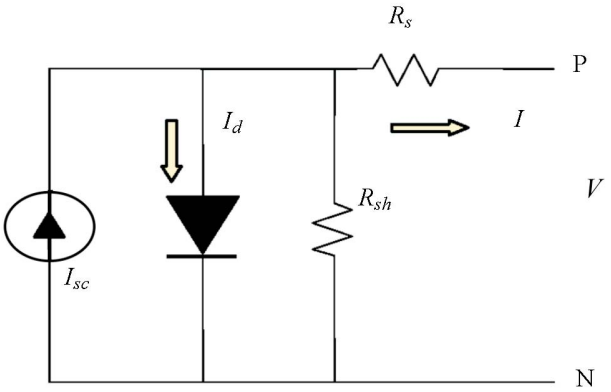

Figure 1. Equivalent circuit of PV array.

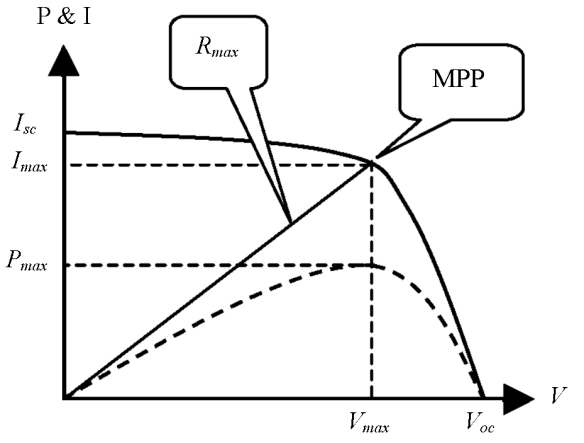

Figure 2. V-I characteristic of a solar cell.

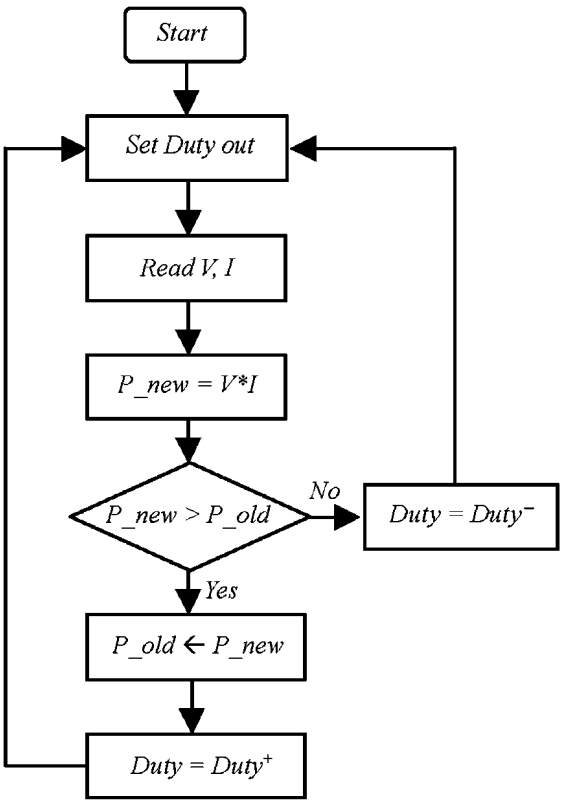

Figure 3. Flow chart of the P&O algorithm.

bation of the solar array voltage, and $Duty^+$ and $Duty^-$ represent the subsequent perturbation in the same or opposite direction, respectively.

4. Three-point Weight Comparision Method

The P&O algorithm compares only two points, which are the current operation point and the subsequent perturbation point, to observe their changes in power and thus decide whether increase or decrease the solar array voltage. The P&O algorithm oscillates around the MPP, resulting in a loss of PV power, especially in cases of rapidly changing solar radiation [6]. Therefore, the three-point weight comparison method is proposed to avoid having to move rapidly the operation point, when the solar radiation is varying quickly or when a disturbance or data reading error occur. Restated, the MPPT can be traced accurately when the solar radiation is stable and power loss is low.

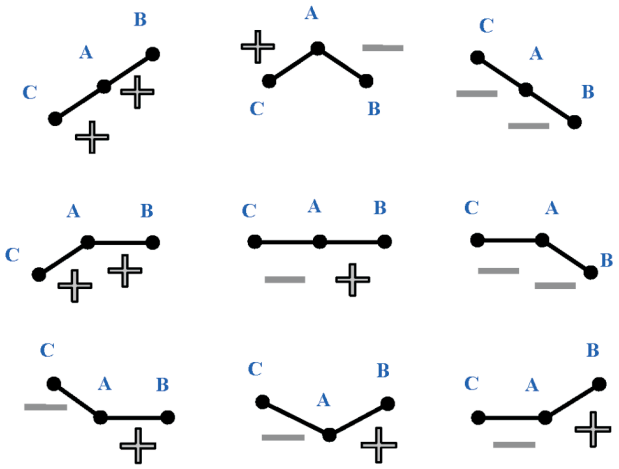

Figure 4. Possible states of the three perturbation points.

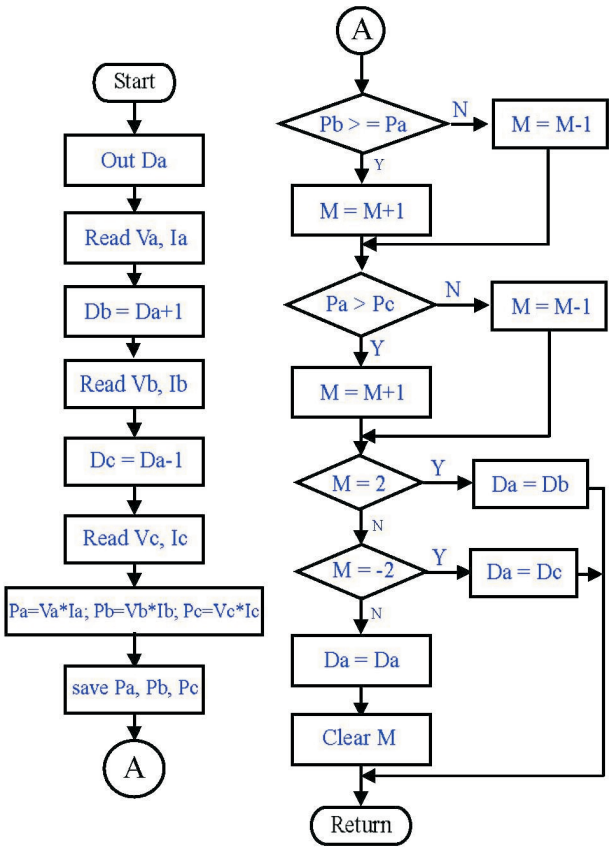

Figure 5. Algorithm for the three-point weight comparison.

The algorithm of the three-point weight comparison is run periodically by perturbing the solar array terminal voltage and comparing the PV output power on three points of the V-P curve. The three points are the current operation point (A), a point, B, perturbed from point A, and a point, C, with doubly perturbed in the opposite direction from point B. Figure 4 depicts the nine possible cases. In these cases, for the point A and B, if the Wattage of point B is greater than or equal to that of point A, the status is assigned a positive weighting. Otherwise, the status is assigned a negative weighting. And, for the point A and C, when the Wattage of point C is smaller than that of point A, the status is assigned a positive weighting. Otherwise, the status is assigned a negative weighting. Of the three measured points, if two are positively weighted, the duty cycle of the converter should be increased. On the contrary, when two are negatively weighted, the duty cycle of the converter should be decreased. In the other cases with one positive and one negative weighting, the MPP is reached or the solar radiation has changed rapidly and the duty cycle is not to be changed. Figure 5 presents a flow chart of the three-point weight comparison algorithm.

5. Configuration of the PV System

Figure 6 shows the system configuration of the proposed PV system. This system consists of a solar array (75 W) with an open voltage of 21 V and a short circuit current of 4.6 A, an A/D and D/A converter, a 20 Ω/100 W resistor as the load, and a control unit on a single-chip. Figure 7 depicts the circuits of the boost converter connected from the output of the solar cell. The power flow is controlled by varying the on/off duty cycle of the

switching. The average output voltages are determined by the Eq. (2) [10].

$$\frac{V_{out}}{V_{in}} = \frac{1}{(1-D)} \tag{2}$$

Where V_{out} and V_{in} are the output and input voltage of the converter and D is the duty cycle of the switch S. The input power of the converter is equal to the output power of the converter if the converter is ideal, yielding the following equations.

$$I_{out} = I_{in} * (1-D) \tag{3}$$

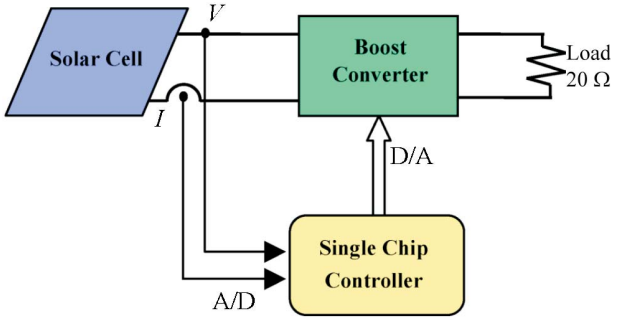

Figure 6. Configuration of the PV system.

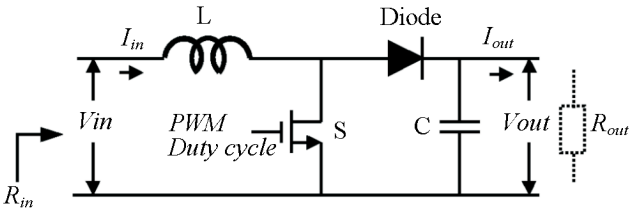

Figure 7. Circuits of the boost converter.

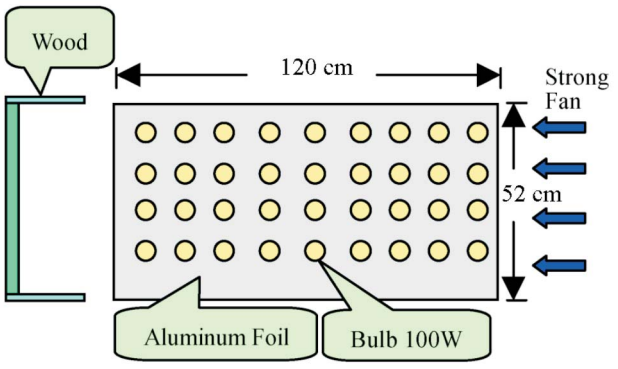

Figure 8. Configuration of the simulated solar source.

$$R_{in} = \frac{V_{in}}{I_{in}} = \frac{V_{out}}{I_{out}}(1-D)^2 = R_{out}(1-D)^2 \tag{4}$$

From Eq. (4), when the load (R_{out}), is fixed, the input resistance R_{in} can be controlled by varying the duty cycle. Therefore, the operating point of the solar cell can be controlled by the duty cycle.

A simulated solar source was established to compare results under the same environmental conditions for various test cases. Figure 8 shows the configuration of the simulated solar source with a maximum energy of 32.68 mA/cm^2.

6. Simulation Results

A prototype MPPT system has been developed using the described method and tested in the laboratory. The PV array gives a 75 W maximum power, a 21 V open-circuit voltage and a close-circuit current of 4.6 A at a solar energy of 1 kW/m^2 and a temperature of 25 °C. The PV array was simulated with two solar energy cases, 32.68 mA/cm^2 (case A) and 12.49 mA/cm^2 (case B) to test the proposed system under specific atmospheric conditions. Figures 9 and 10 plot the V-I and V-P curves under the two cases at 65 °C.

Figures 11 and 12 show the output voltage (CH1) and the current (CH2) waveforms. The solar energy is changed form A to B in Figure 11. In Figure 12, the solar energy is changed form B to A. In the case A, the MPP is 13.65 V, 3.76 A and 51.324 W. And for the case B, the MPP is 16.14 V, 1.32 A and 21.305 W. From Figure 11

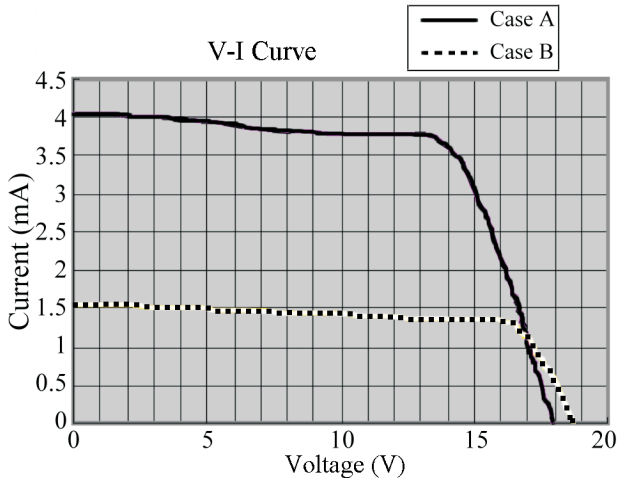

Figure 9. V-I curve under the cases A and B at 65 °C.

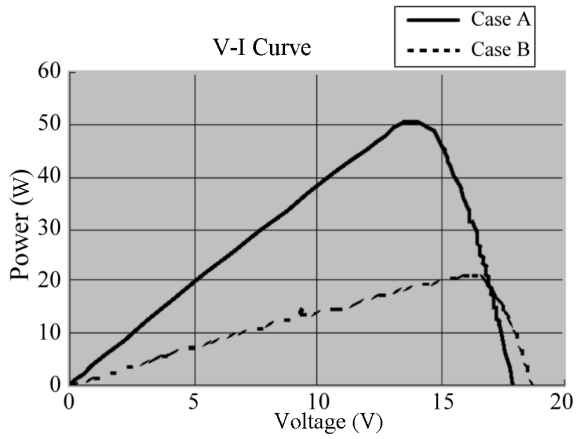

Figure 10. V-P curve under the cases A and B at 65 °C.

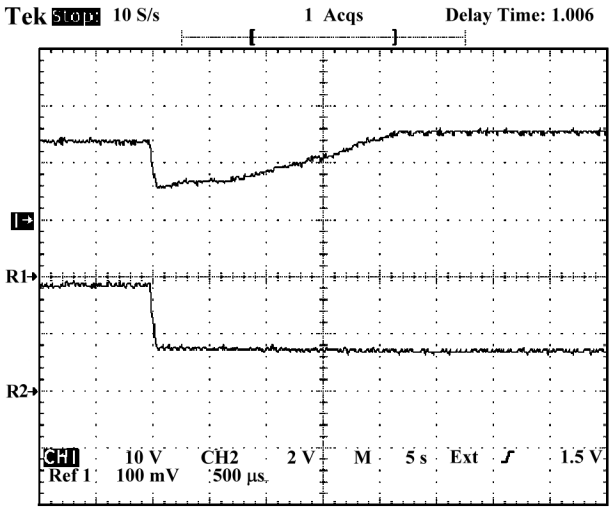

Figure 11. Output voltage and current of the PV array. (The solar energy is changed from A to B.)

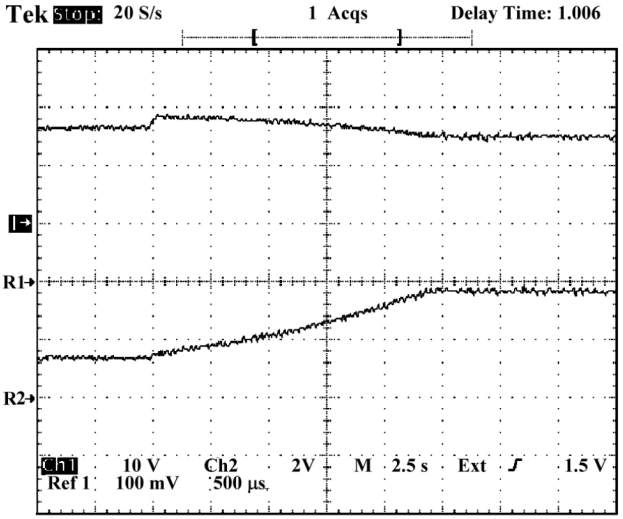

Figure 12. Output voltage and current of the PV array. (The solar energy is changed from B to A.)

and 12, it is noted that the operating points of a PV array are different under the two cases.

Figure 13 displays the waveforms of the voltage (CH1), current (CH2) and power (CHM) with uniformly changing energy from zero to B and finally to A, and then decreasing to B and finally to zero at the same rate. Figure 13 reveals that the rate of change of voltage and current differ. In the beginning, the voltage of the PV increases rapidly with the solar energy but the current changes slowly. As the solar energy increases further, the voltage changes slowly, and the current increases fast. When the temperature increases, the voltage decreases.

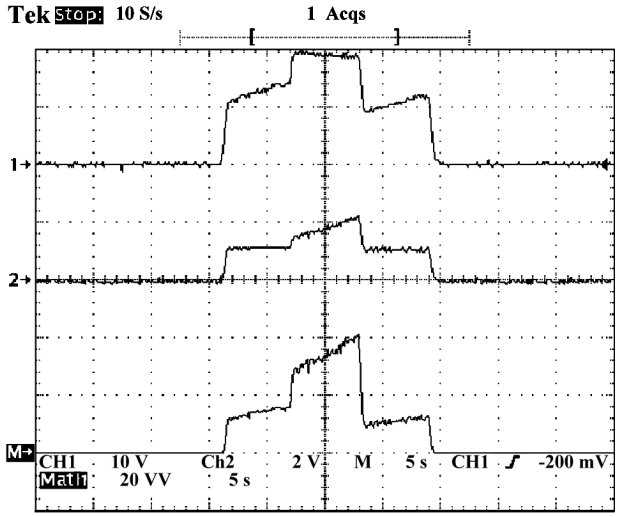

Figure 13. Wave form of the voltage, current and power as the solar energy changes uniformly from zero to B and finally to A, and then decreases to B and finally to zero, at the same rate.

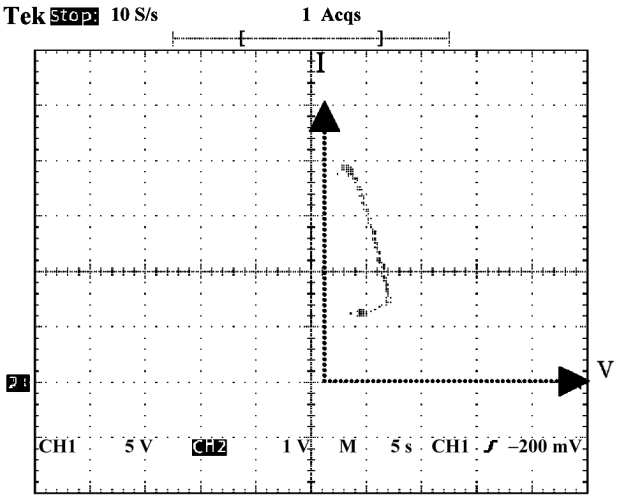

Figure 14. Trace of V-I curve under as the solar energy increases slowly from B to A.

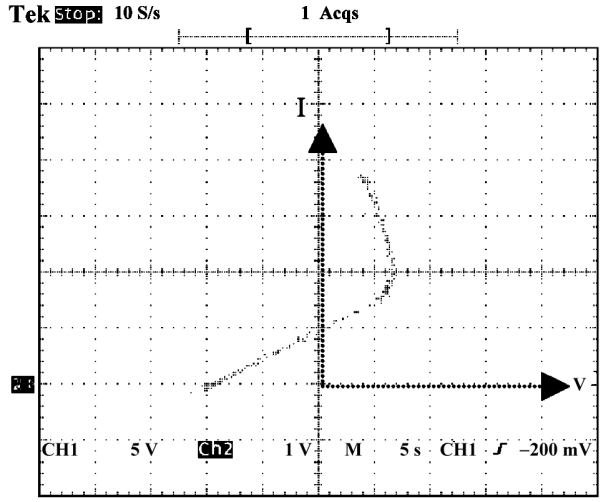

Figure 15. Trace of V-I curve as the solar energy increases slowly from 0 to A.

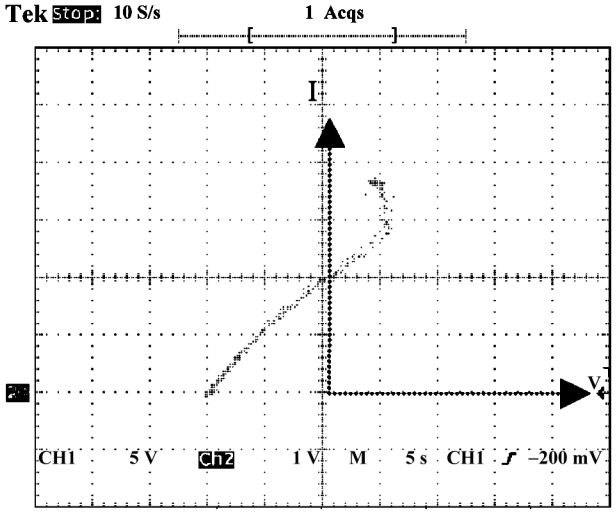

Figure 16. Trace of V-I curve as the solar energy increases fast from B to A.

These trends satisfy the characteristic of solar cells.

Figure 14 depicts the V-I trace as the solar energy increase slowly from B to A. Figure 15 displays the V-I curve as the solar energy increases slowly from zero to A. Figure 16 presents the V-I trace under as the solar energy increases rapidly from zero to A. Figures 14 to 16, show that, regardless of how the luminous flux changes, the output power point is well tracked, and stays on the MPP.

7. Conclusion

This paper proposed a single and robust algorithm for MPPT. Moreover, the three-point weight point comparison method was developed to avoid the oscillation problem in the traditional P&O algorithm. This work also developed a low-cost hardware system. The system includes a boot converter and a micro controller on a single-chip unit, which controls the converter directly according to the PV array output power measurements. The experimental tests verified the tracking efficiency.

Acknowledgment

The authors would like to thank the National Science Council of the Republic of China for financially supporting this research under Contract No. NSC 90-2213-E-032-018.

Reference

[1] Ibrahim, H. E.-S. A. and Houssiny, F. F., "Microcomputer Controlled Buck Regulator for Maximum Power Point Tracker for DC Pumping System Operates from Photovoltaic System," *Proceedings of the IEEE International Fuzzy Systems Conference*, August 22–25, Vol. 1, pp. 406–411 (1999).

[2] Midya, P., Kerin, P. T., Turnbull, R. J., Reppa, R. and Kimball, J., "Dynamic Maximum Power Point Tracker for Photovoltaic Applications," *Proceedings of the IEEE Power Electronics Specialists Conference, PESC*, Vol. 2, pp. 1710–1716 (1996).

[3] Enslin, J. H. R. and Snyman, D. B., "Simplified Feed-Forward Control of the Maximum Power Pont in PV Installations," *Proceedings of the IEEE International Conference on Power Electronics Motion Control*, Vol. 1, pp. 548–553 (1992).

[4] Bose, B. K., Szczeny, P. M. and Steigerwald, R. L., "Microcomputer Control of a Residential Photovoltaic Power Conditioning System," *IEEE Transactions on Industrial Electronics*, Sept./Oct., Vol. IA-21, pp. 1182–1191 (1985).

[5] Kuo, Y. C., Liang, T. J. and Chen, F. C., "Novel Maximum-Power-Point-Tracking Controller for Photovoltaic Energy Conversion System," *IEEE Transactions on Industrial Electronics*, Vol. 48, pp. 594–601 (2001).

[6] Koutroulis, E., Kalaitzakis, K. and Voulgaris, N. C., "Development of a Microcontroller-Based Photovoltaic Maximum Power Point Tracking Control System,"

IEEE Transactions on Power Electronics, Vol. 16, pp. 46–54 (2001).

[7] Hussein, K. H., Muta, I., Hoshino, T. and Osakada, M., "Maximum Photovoltaic Power Tracking: an Algorithm for Rapidly Changing Atmospheric Condition," *IEE Proc.-Gener. Transm. Distrib*, Vol. 142, pp. 59–64 (1995).

[8] Matsui, M., Kitano, T., Xu, D. H. and Yang, Z. Q., "A New Maximum Photovoltaic Power Tracking Control Scheme Based on Power Equilibrium at DC Link," *Proceedings of the IEEE Industrial Electronics Society 25th Annual Conference*, pp. 804–809 (1999).

[9] Bodur, M. and Ermis, M., "Maximum Power Point Tracking for Low Power Photovoltaic Solar Panels," *Proceedings of the IEEE Electro Technical Conference*, pp. 758–761 (1994).

[10] Simoes, M. G., Franceschetti, N. N. and Friedhofer, M., "A Fuzzy Logic Based Photovoltaic Peak Power Tracking Controller," *Proceedings of the IEEE International Symposium on Industrial Electronics*, pp. 300–325 (1998).

[11] Mahmoud, A. M. A., Mashaly, H. M., Kandil, S. A., Khashab, H. E. and Nashed, M. N. F., "Fuzzy Logic Implementation for Photovoltaic Maximum Power Tracking," *Proceedings of the IEEE International Workshop on Robot and Human Interactive Communication*, Osaka, Japan, 27–29 (2000).

Manuscript Received: Dec. 10, 2004
Accepted: Mar. 14, 2005